Electronic Supporting Information for

Time-evolved, far-red, circularly polarised luminescent polymer aggregates endowed with sacrificial Si–Si bond helical polymers

Michiya Fujiki[a,*] and Shosei Yoshimoto[a]

[a] Graduate School of Materials Science, Nara Institute of Science and Technology, 8916-5 Takayama, Ikoma, Nara 630-0192, Japan. E-mail: fujikim@ms.naist.jp

Contents

General conditions of chiroptical experiments

Measurement conditions: CD/UV-VIS-NIR: scanning rate: 100 nm/min, PMT response time : 2 sec, bandwidth 2.0 nm, data sampling 1.0 nm interval, sensitivity: ±1000 mdeg. CPL/PL: scanning rate: 100 nm/min, PMT response time : 1 sec, bandwidth 1200 μm for excitation (400 nm), bandwidth 1500 μm for emission, data sampling 1.0 nm, three times scanning.

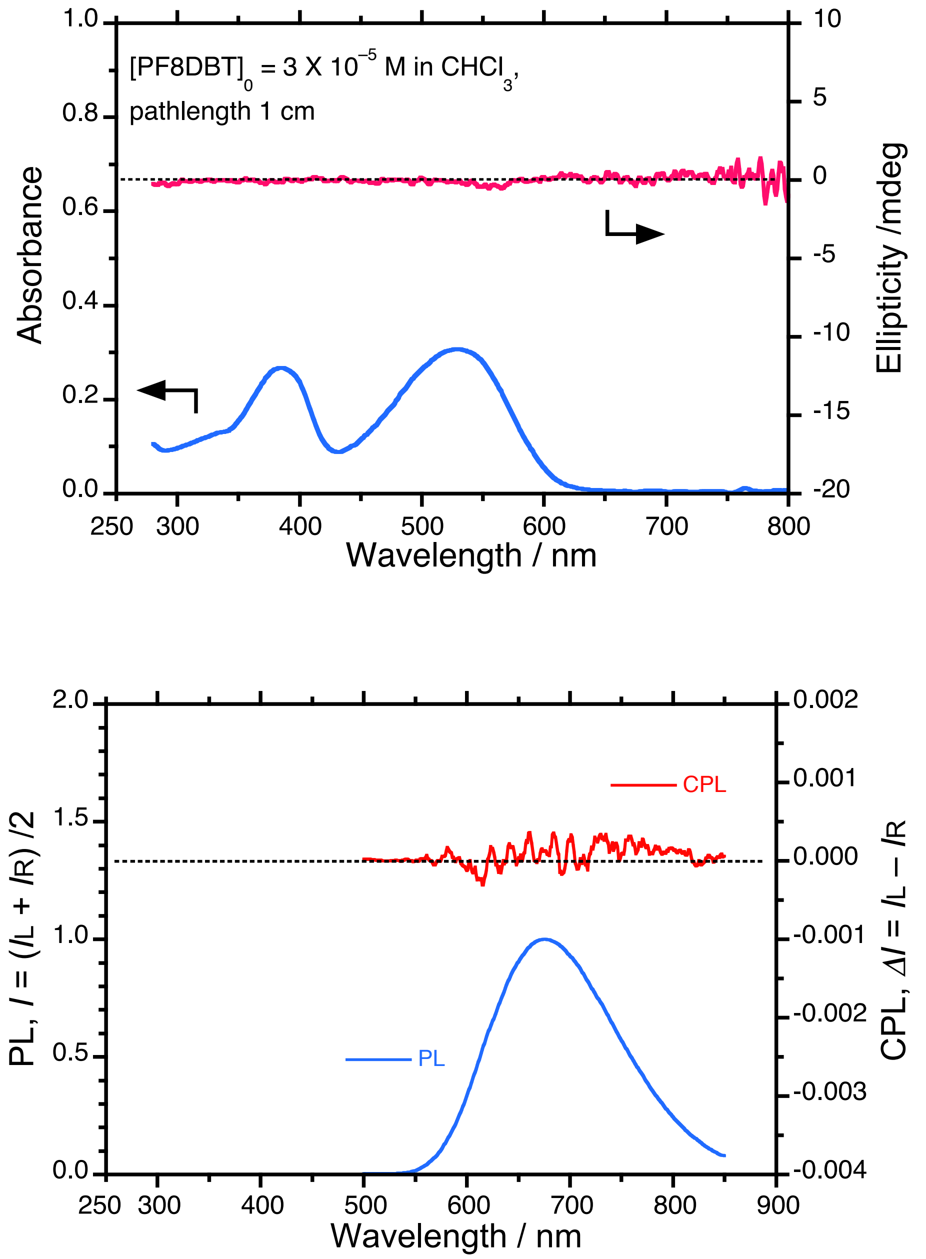

Figure S1. CD/UV-VIS-NIR/CPL/PL (excited at 400 nm) spectra of **PF8DBT** (3 x 10^{-5} M (as repeating unit)) and path length of 1.0 cm dissolved in pure CHCl$_3$ at room temperature.

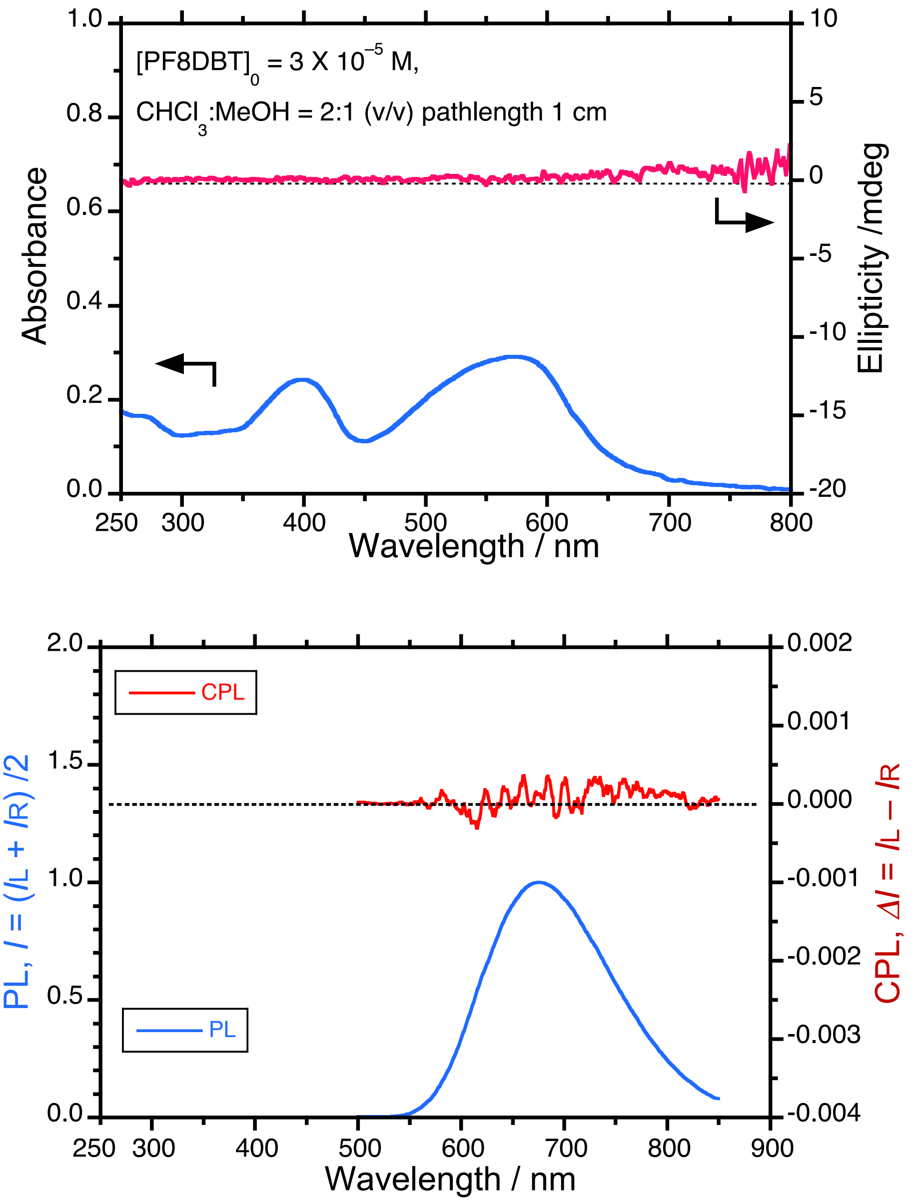

Figure S2. CD/UV-VIS-NIR/CPL/PL (excited at 400 nm) spectra of **PF8DBT** homo- aggregates (3 x 10^{-5} M (as repeating unit) and path length of 1.0 cm in CHCl$_3$: MeOH (2/1 (v/v)) at room temperature.

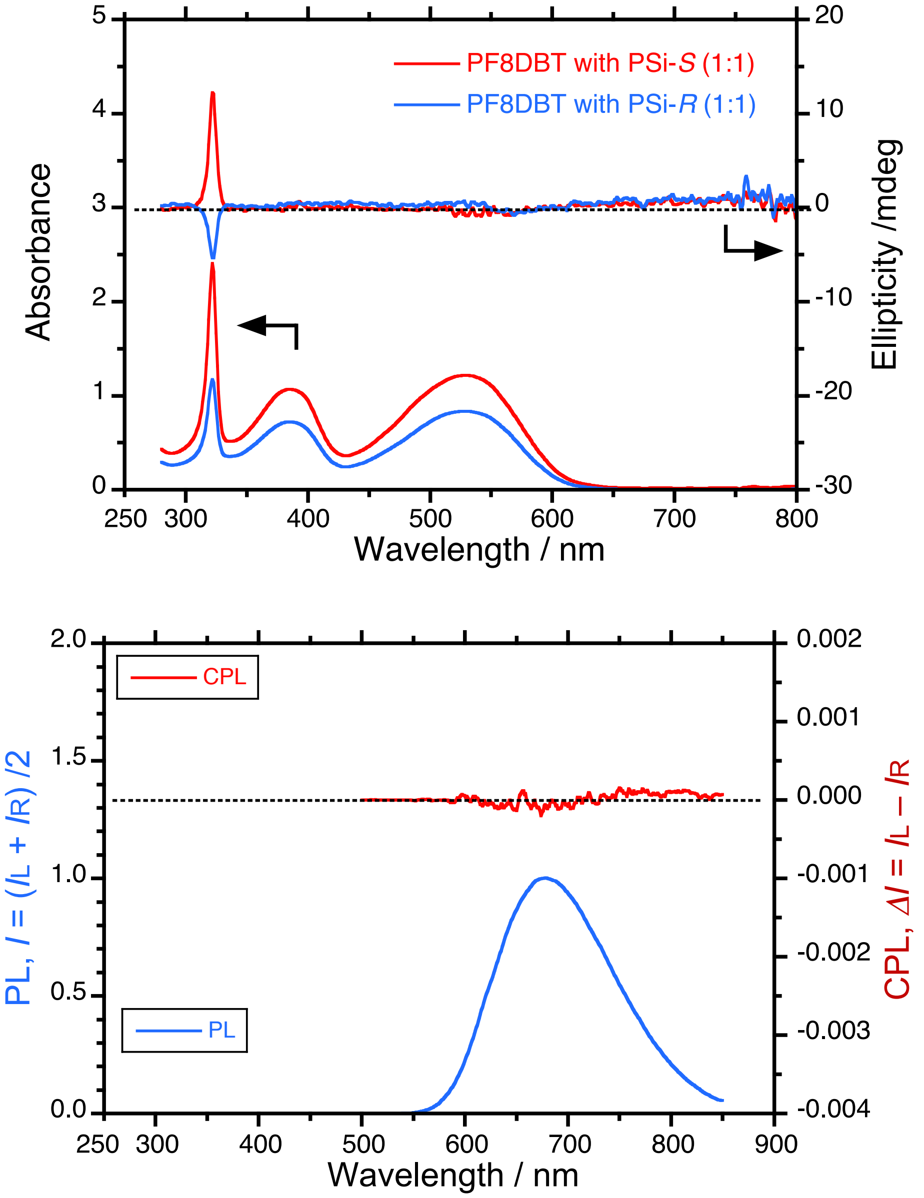

Figure S3. CD/UV-VIS-NIR/ CPL/PL (excited at 400 nm) spectra of **PF8DBT** with **PSi-*S*** or **PSi-*R*** (1:1 in molar ratio as of repeating unit). ([**PF8DBT**]$_0$ = [**PSi-*S*** or **PSi-*R***]$_0$ = 5 x 10^{-5} M, path length of 0.5 cm dissolved in pure CHCl$_3$ at room temperature.

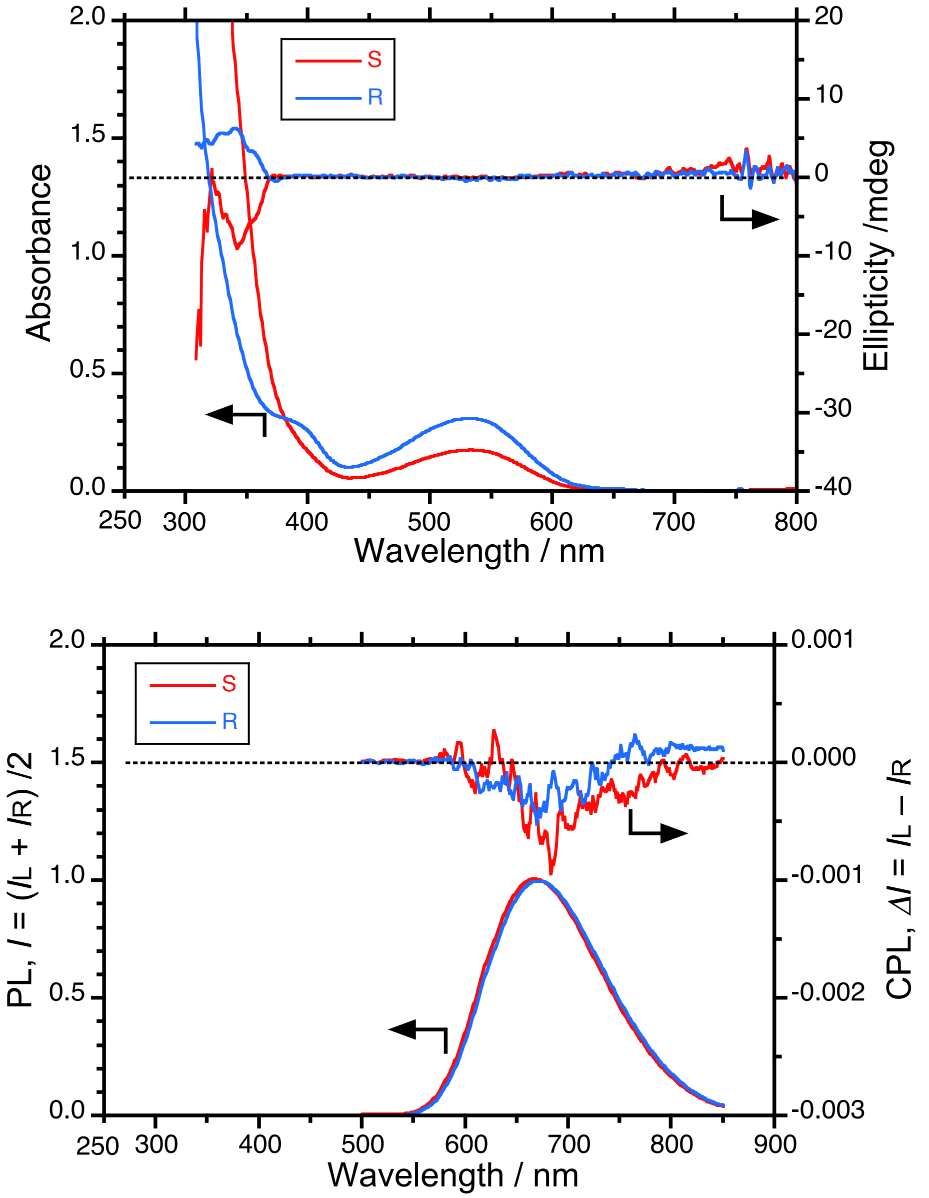

Figure S4. CD/UV-VIS-NIR/CPL/PL (excited at 400 nm) spectra of **PF8DBT** (3 x 10^{-5} M (as repeating unit) and path length of 1.0 cm dissolved in (*S*)- or (*R*)-limonene:$CHCl_3$ = 1/2 (v/v) at room temperature.

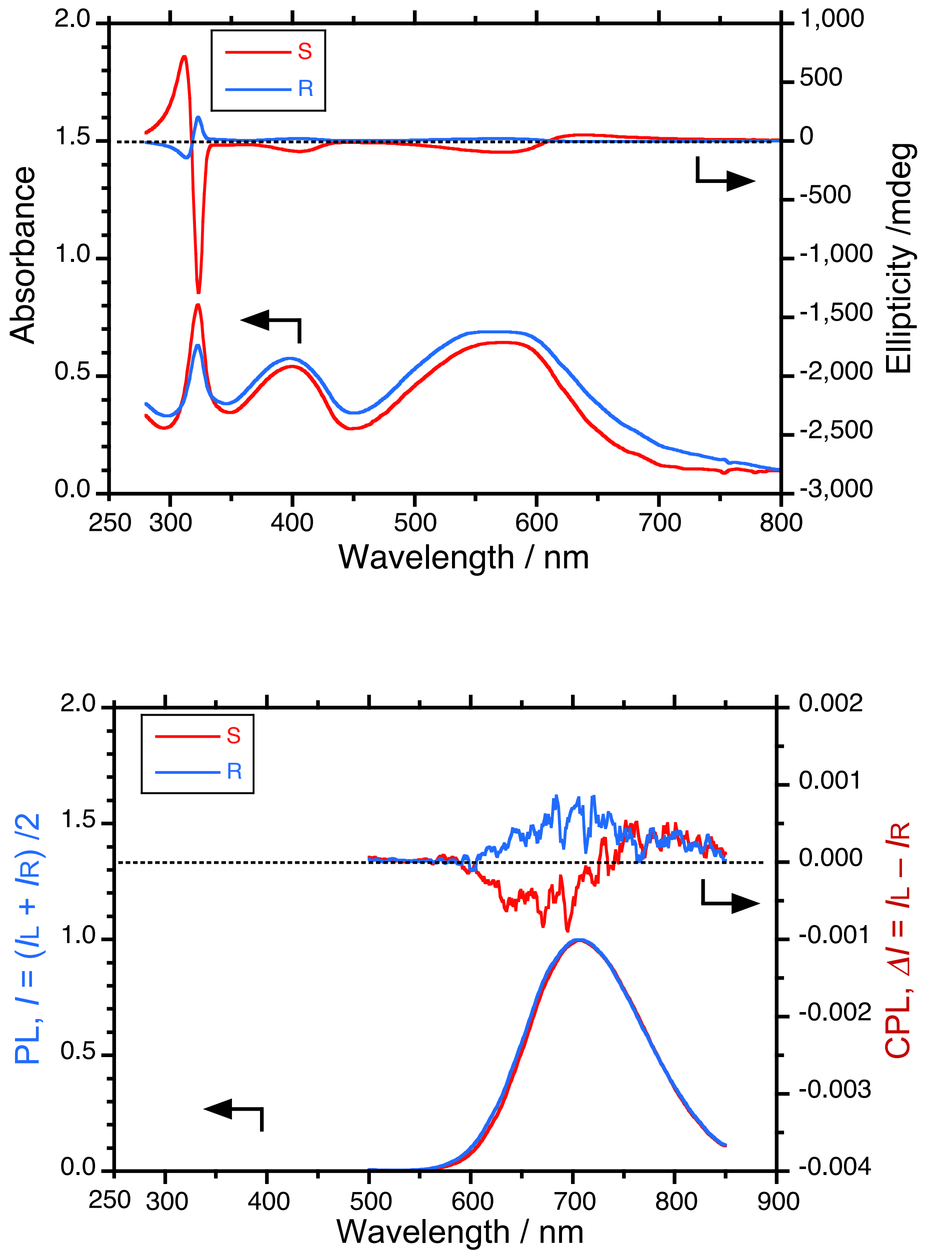

Figure S5. CD/UV-VIS-NIR/ CPL/PL (excited at 400 nm) spectra of **PF8DBT** hetero-aggregate with **PSi-*S*** or **PSi-*R*** (1/1 in molar ratio as of repeating unit). ([**PF8DBT**]$_0$ = [**PSi-*S*** or **PSi-*R***]$_0$ = 3 x 10^{-5} M, path length of 0.5 cm in $CHCl_3$:MeOH = 1/1 (v/v) at room temperature.

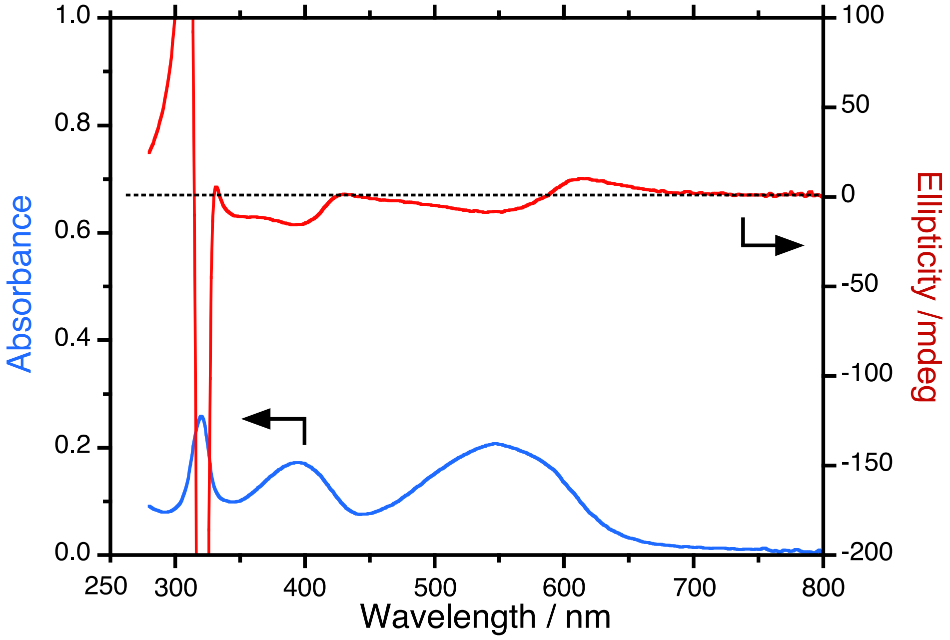

Figure S6. CD/UV-VIS-NIR/ CPL/PL (excited at 400 nm) spectra of **PF8DBT** hetero-aggregate with **PSi-*S*** (1/1 in molar ratio as of repeating unit). ([**PF8DBT**]$_0$ = [**PSi-*S***]$_0$ = 2 x 10^{-5} M as of final centration, path length of 0.5 cm in $CHCl_3$:MeOH = 2/1 (v/v) at room temperature.

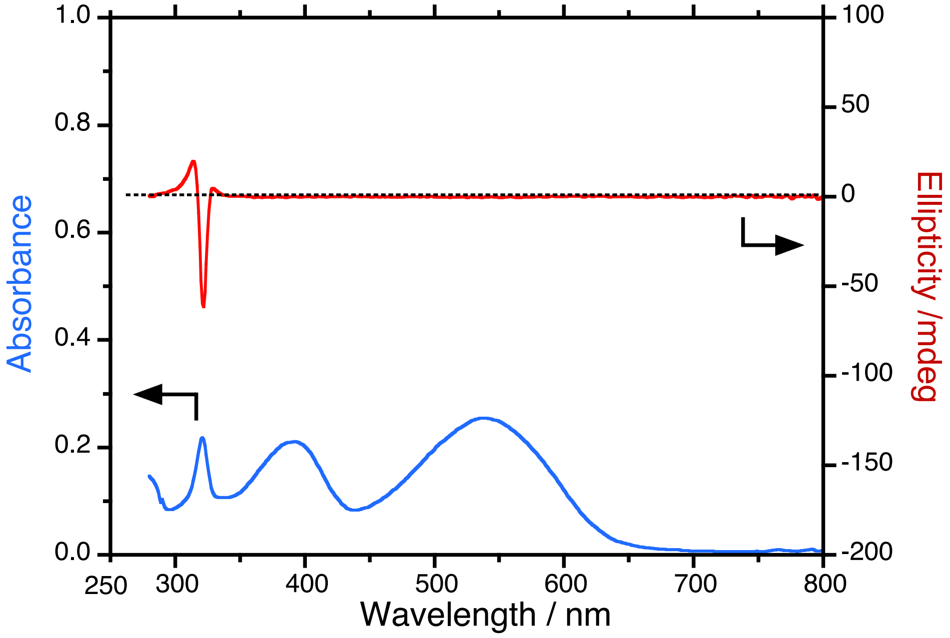

Figure S7. CD/UV-VIS-NIR/ CPL/PL (excited at 400 nm) spectra of **PF8DBT** hetero- aggregate with **PSi-*S*** (1/1 in molar ratio as of repeating unit). ([**PF8DBT**]$_0$ = [**PSi-*S***]$_0$ = 2 x 10^{-5} M as of final centration, path length of 0.5 cm in tetrahydrofuran:MeOH = 2/1 (v/v) at room temperature.

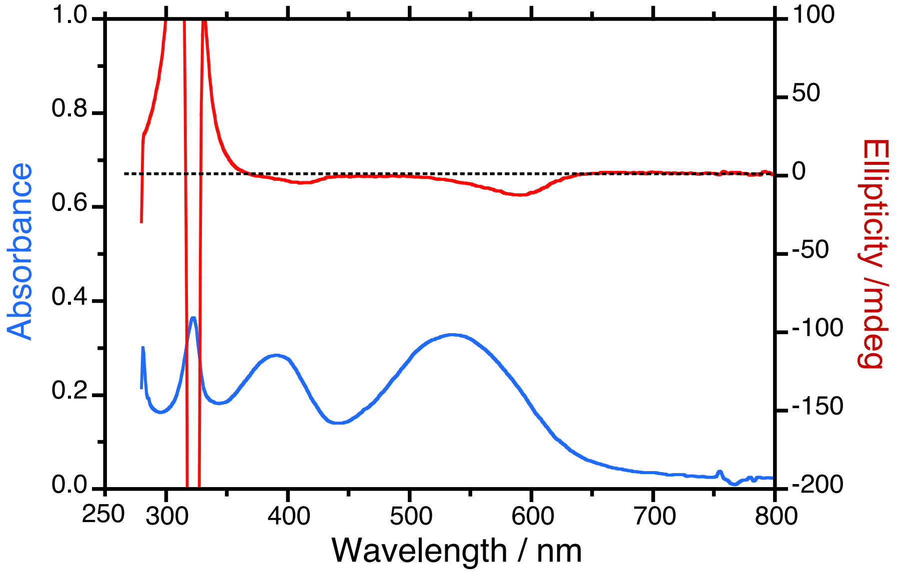

Figure S8. CD/UV-VIS-NIR/ CPL/PL (excited at 400 nm) spectra of **PF8DBT** hetero-aggregate with **PSi-*S*** (1/1 in molar ratio as of repeating unit). ([**PF8DBT**]$_0$ = [**PSi-*S***]$_0$ = 2 x 10^{-5} M as of final centration, path length of 0.5 cm in toluene:MeOH = 2/1 (v/v) at room temperature.

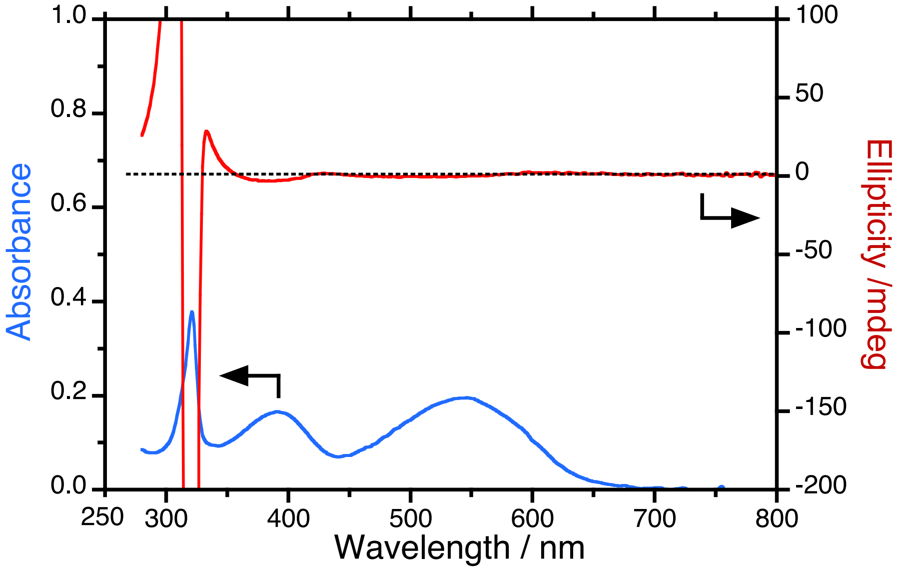

Figure S9. CD/UV-VIS-NIR/ CPL/PL (excited at 400 nm) spectra of **PF8DBT** hetero-aggregate with **PSi-*S*** (1/1 in molar ratio as of repeating unit). ([**PF8DBT**]$_0$ = [**PSi-*S***]$_0$ = 2 x 10^{-5} M as of final centration, path length of 0.5 cm in toluene: ethanol = 2/1 (v/v) at room temperature.

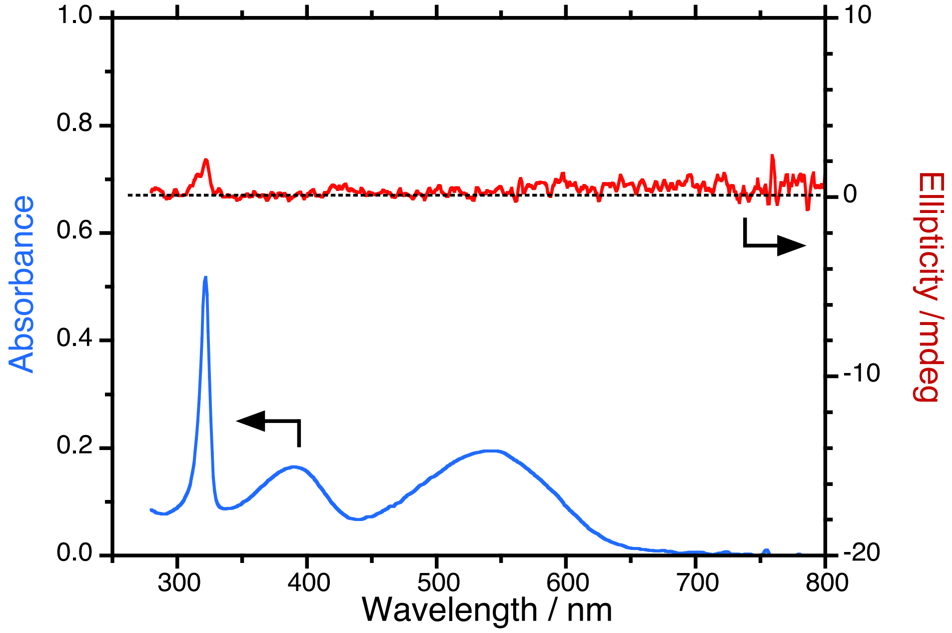

Figure S10. CD/UV-VIS-NIR/ CPL/PL (excited at 400 nm) spectra of **PF8DBT** hetero-aggregate with **PSi-*S*** (1/1 in molar ratio as of repeating unit). ([**PF8DBT**]$_0$ = [**PSi-*S***]$_0$ = 2 x 10^{-5} M as of final centration, path length of 0.5 cm in toluene: 2-propanol = 2/1 (v/v) at room temperature.

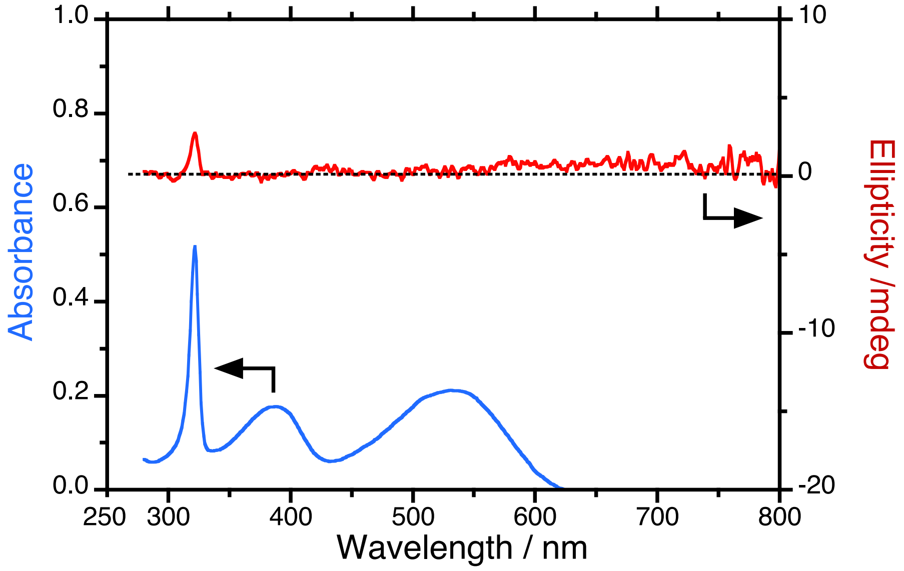

Figure S11. CD/UV-VIS-NIR/ CPL/PL (excited at 400 nm) spectra of **PF8DBT** hetero-aggregate with **PSi-*S*** (1/1 in molar ratio as of repeating unit). ([**PF8DBT**]$_0$ = [**PSi-*S***]$_0$ = 2 x 10^{-5} M as of final centration, path length of 0.5 cm in toluene: *n*-hexane = 2/1 (v/v) at room temperature.

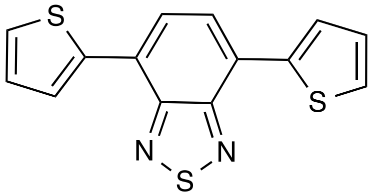

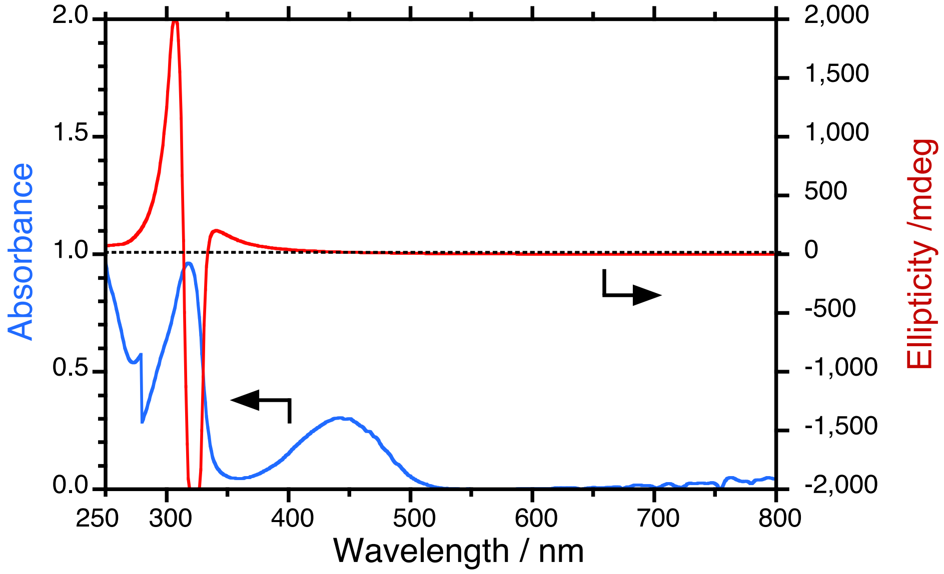

Figure S12. CD/UV-VIS-NIR spectra of **DBT** hetero-aggregate with **PSi-*S*** ([**DBT**]$_0$ = [**PSi-*S***]$_0$ = 2 x 10^{-5} M as of final centration, path length of 0.5 cm in $CHCl_3$: MeOH = 2/1 (v/v) at room temperature.

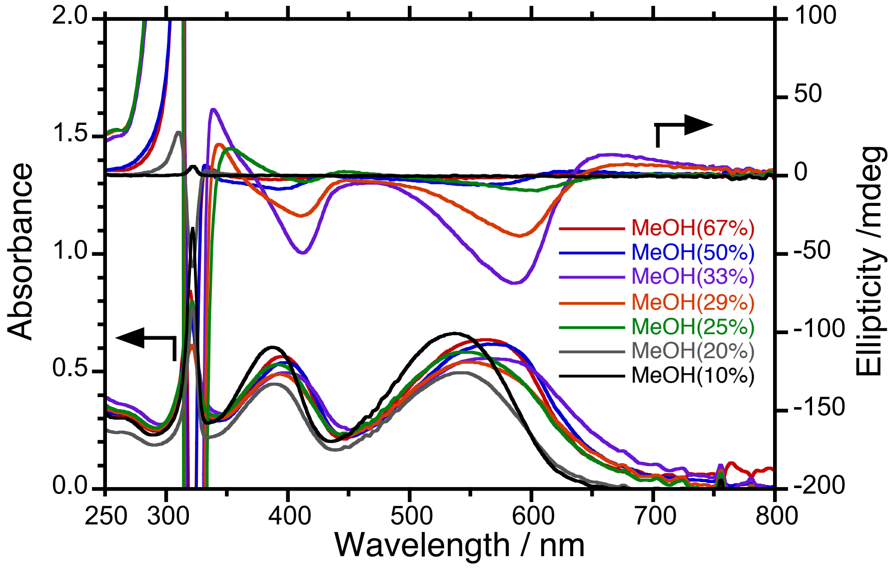

Figure S13. CD/UV-VIS-NIR spectra of **PF8DBT** hetero-aggregate with **PSi-*S*** ([**DBT**]$_0$ = [**PSi-*S***]$_0$ = 2 x 10^{-5} M as of final centration, path length of 0.5 cm as a function of volume fraction of MeOH relative to total 3.0 mL of MeOH-CHCl$_3$ cosolvents at room temperature.

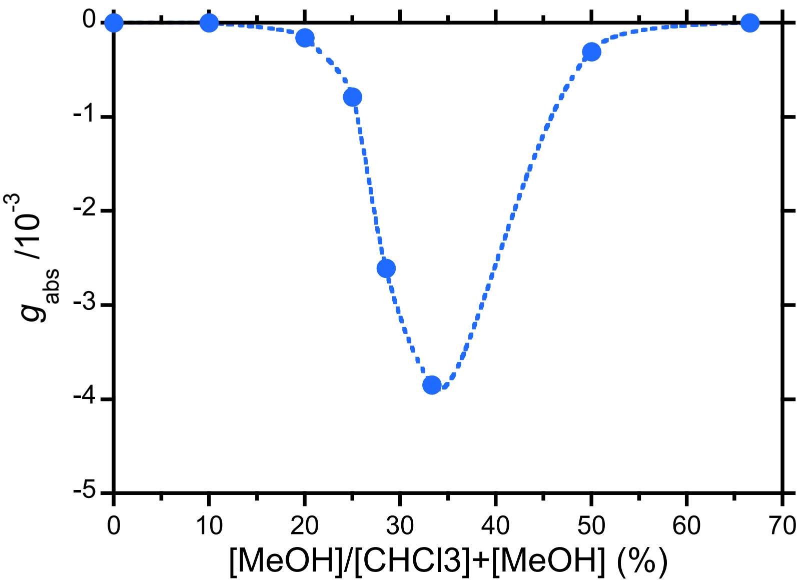

Figure S14. The g_{abs} value of **PF8DBT** hetero-aggregate with **PSi-*S*** ([**PF8DBT**]$_0$ = [**PSi-*S***]$_0$ = 2 x 10^{-5} M as of final centration, path length of 0.5 cm) as a function of volume fraction of MeOH relative to total 3.0 mL of CHCl$_3$-MeOH cosolvents at room temperature.

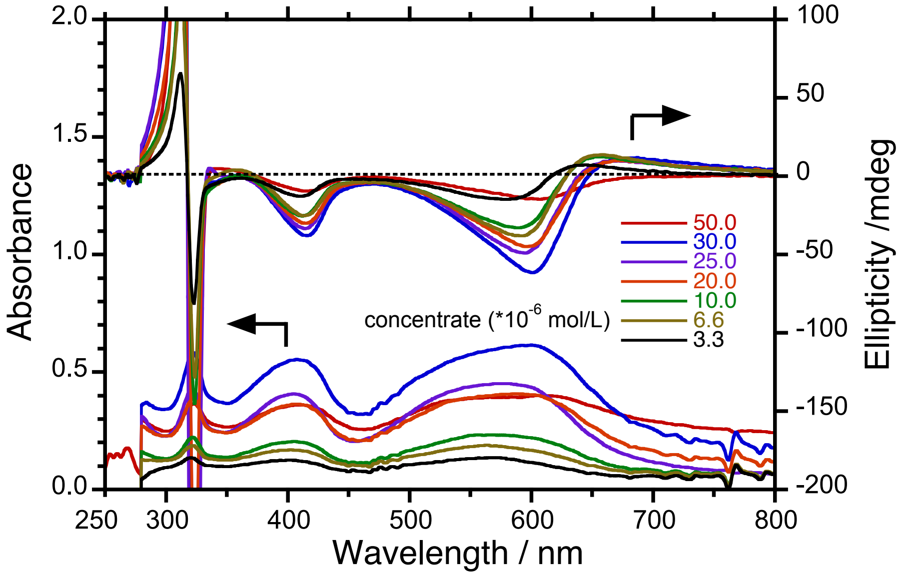

Figure S15. CD/UV-VIS-NIR spectra of **PF8DBT** hetero-aggregate with **PSi-*S*** ([**DBT**]$_0$ = [**PSi-*S***]$_0$ as of final centration, path length of 0.5 cm) as a function of [**PF8DBT**]$_0$ = [**PSi-*S***]$_0$ in $CHCl_3$: MeOH cosolvents = 2:1 (v/v) at room temperature.

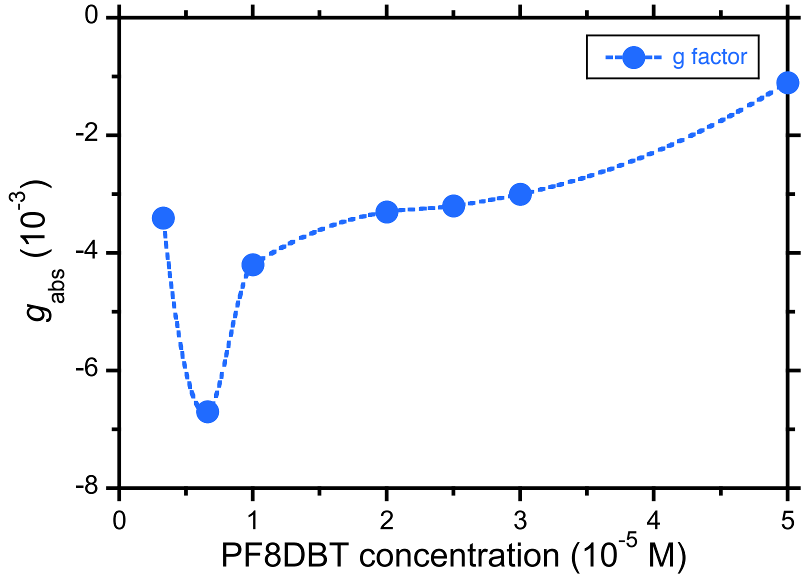

Figure S16. The g_{abs} value of **PF8DBT** hetero-aggregate with **PSi-*S*** ([**DBT**]$_0$ = [**PSi-*S***]$_0$, path length of 0.5 cm) as a function of [**PF8DBT**]$_0$ = [**PSi-*S***]$_0$ in $CHCl_3$: MeOH cosolvents = 2:1 (v/v) at room temperature.

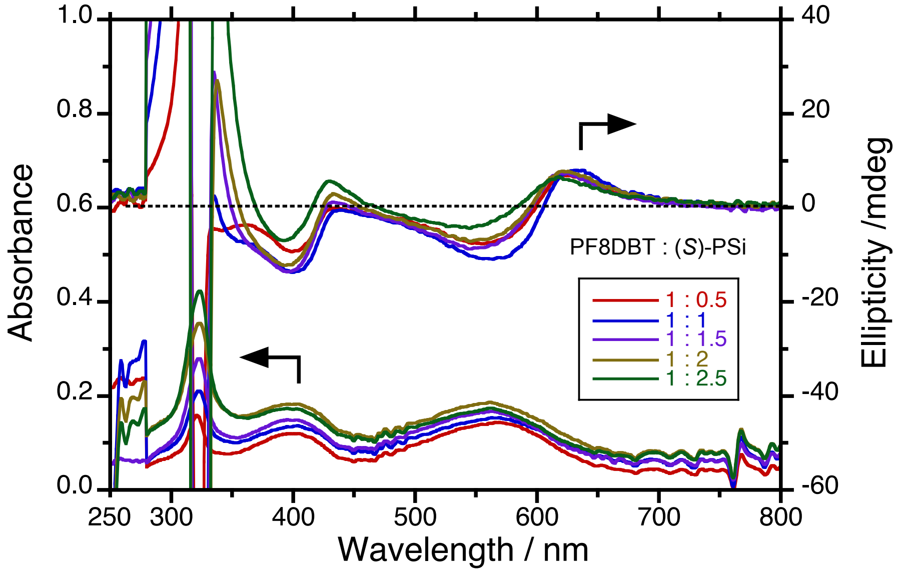

Figure S17. CD/UV-VIS-NIR spectra of **PF8DBT** hetero-aggregates with **PSi-*S*** ([**DBT**]$_0$ = [**PSi-*S***]$_0$, path length of 0.5 cm) as a function of ratio of [**PF8DBT**]$_0$ to [**PSi-*S***]$_0$ in CHCl$_3$: MeOH cosolvents = 2:1 (v/v) at room temperature.

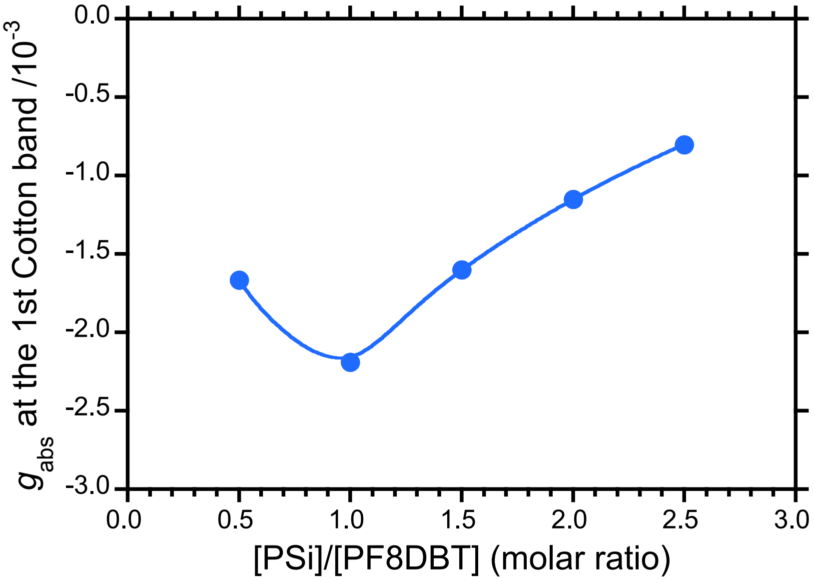

Figure S18. The g_{abs} value of **PF8DBT** hetero-aggregates with **PSi-*S*** ([**F8DBT**]$_0$ = 6.6 x 10^{-5} M as of final concentration, path length of 0.5 cm) as a function of ratio of [**PSi-*S***]$_0$ to [**F8DBT**]$_0$ in CHCl$_3$: MeOH cosolvents = 2:1 (v/v) at room temperature.

FL30°-DBT30°-30°-FL30°

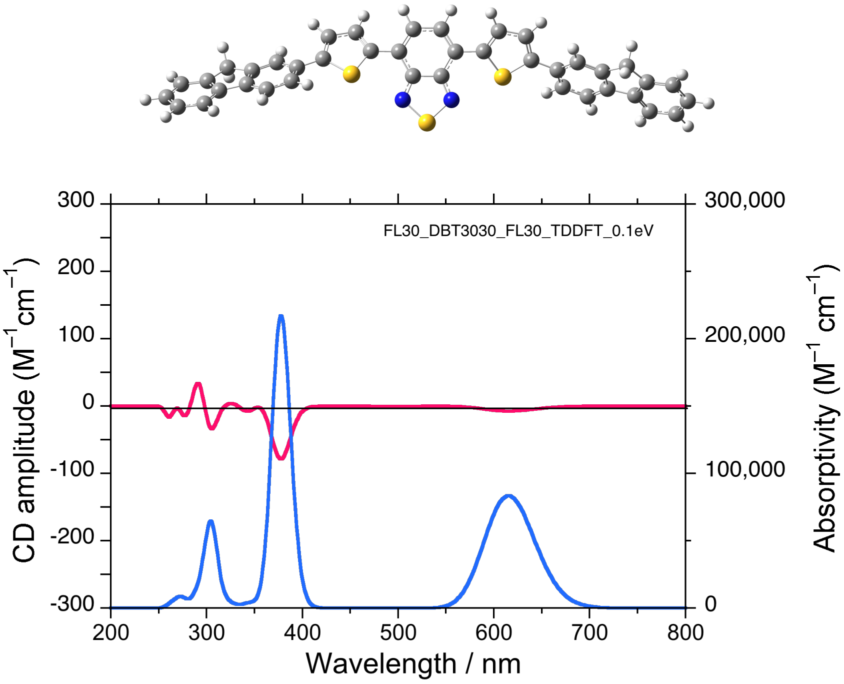

Figure S19. The simulated CD and UV-VIS-NIR spectra of **FL30°-DBT30°-30°-FL30°** of syn-syn **FDBTF** rotamer.

FL150°-DBT30°-30°-FL150°

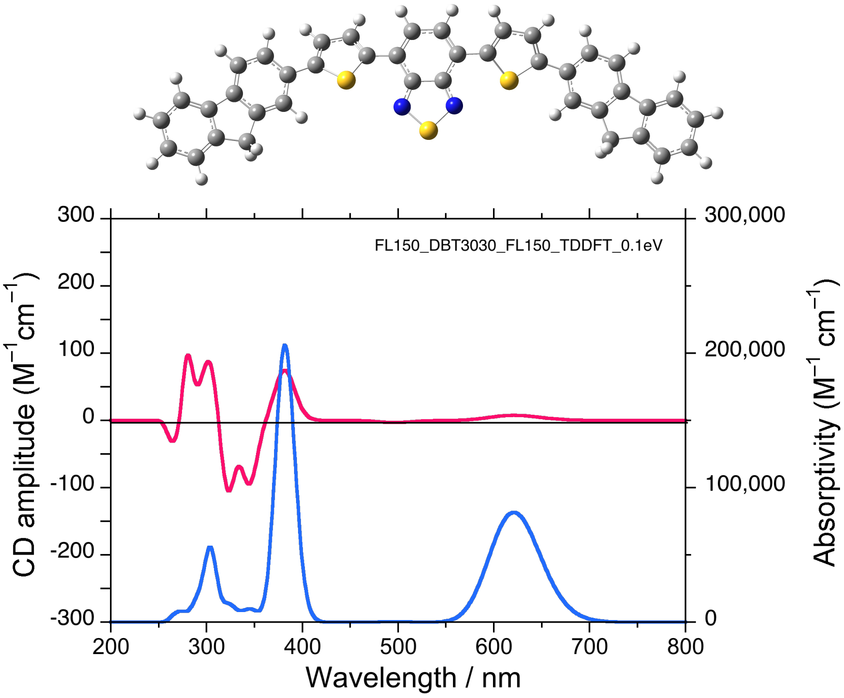

Figure S20. The simulated CD and UV-VIS-NIR spectra of **FL150°-DBT30°-30°-FL150°** of syn-syn **FDBTF** rotamer.

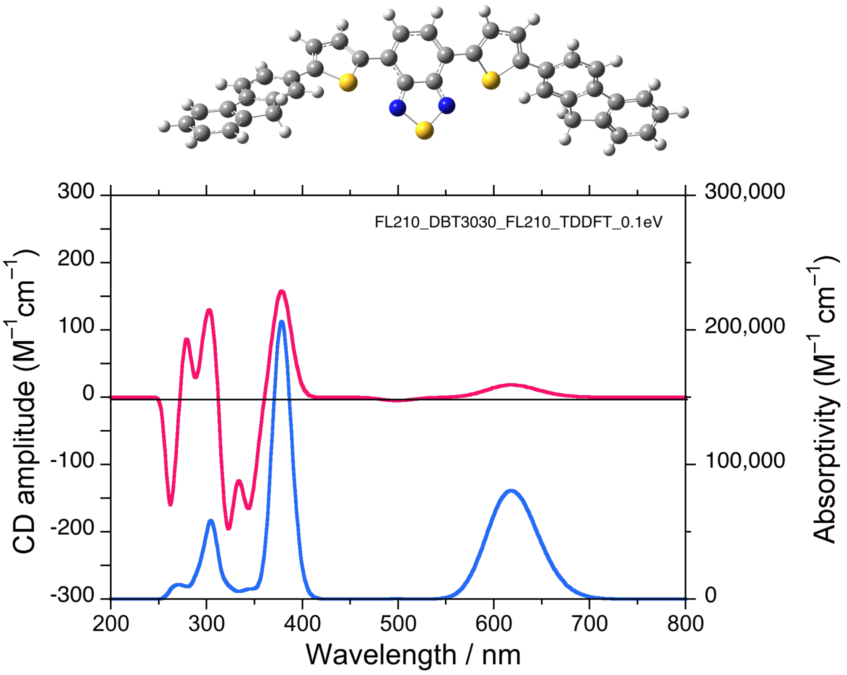
FL210°-DBT30°-30°-FL210°

Figure S21. The simulated CD and UV-VIS-NIR spectra of **FL210°-DBT30°-30°-FL210°** of syn-syn **FDBTF** rotamer.

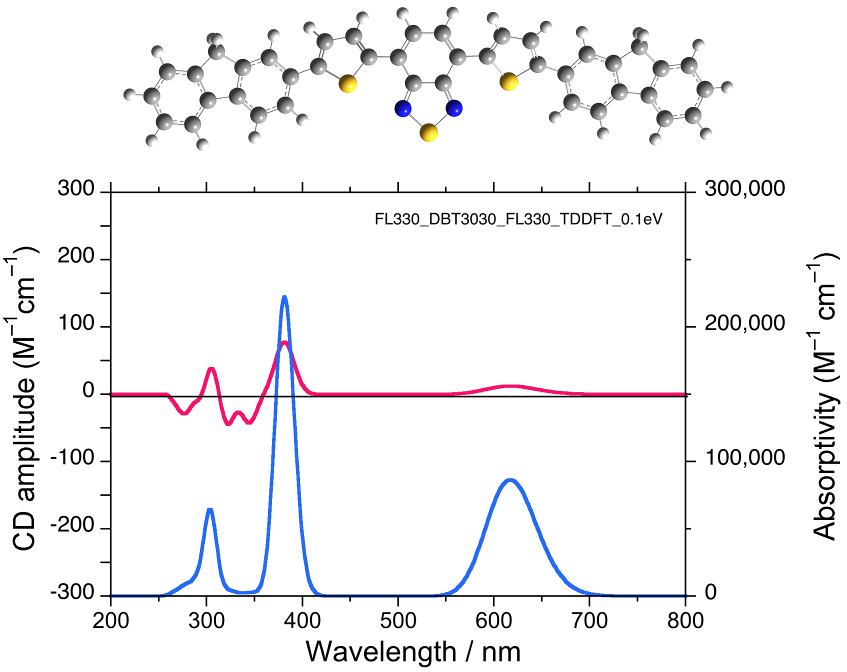
FL330°-DBT30°-30°-FL330°

Figure S22. The simulated CD and UV-VIS-NIR spectra of **FL330°-DBT30°-30°-FL330°** of syn-syn **FDBTF** rotamer.

FL30°-DBT160°160°-FL30°: The most stable

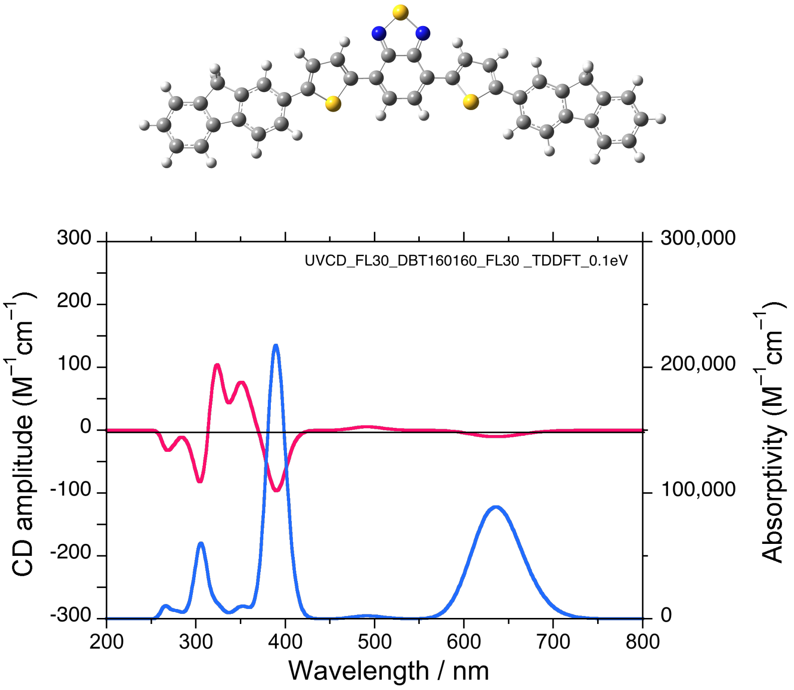

Figure S23. The simulated CD and UV-VIS-NIR spectra of **FL30°-DBT160°-160°-FL30°** of the most anti-anti **FDBTF** rotamer.

FL150°-DBT160°160°-FL150°

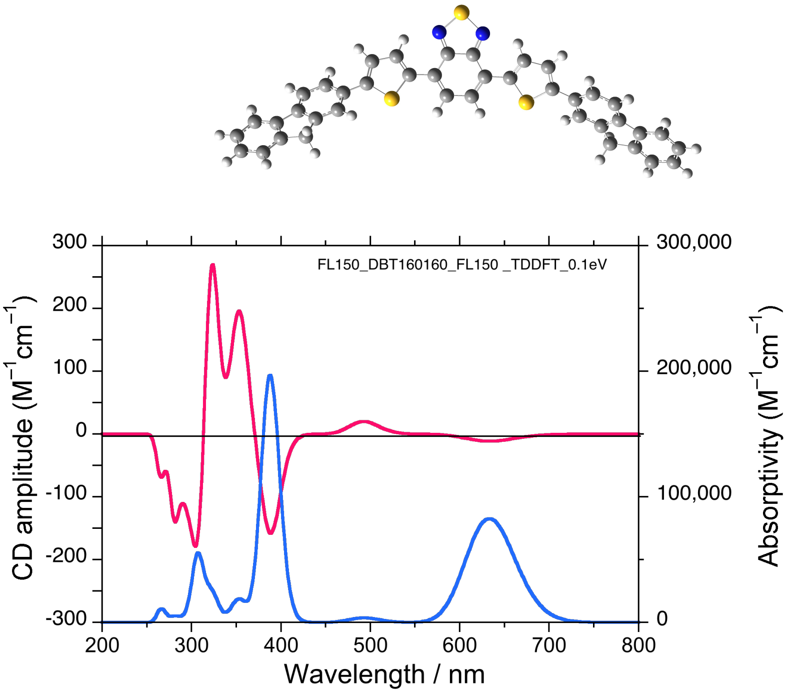

Figure S24. The simulated CD and UV-VIS-NIR spectra of **FL150°-DBT160°-160°-FL150°** of anti-anti **FDBTF** rotamer.

FL210°-DBT160°160°-FL210°

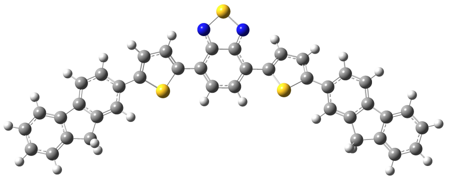

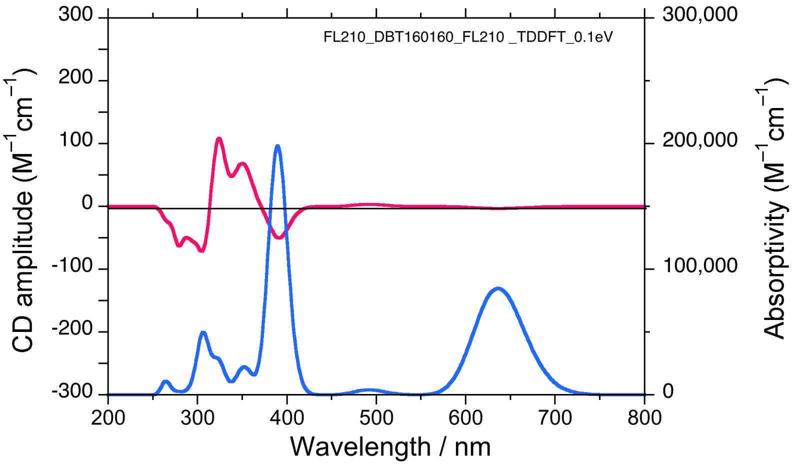

Figure S25. The simulated CD and UV-VIS-NIR spectra of **FL210°-DBT160°-160°-FL210°** of anti-anti **FDBTF** rotamer.

FL330°-DBT160°160°-FL330°

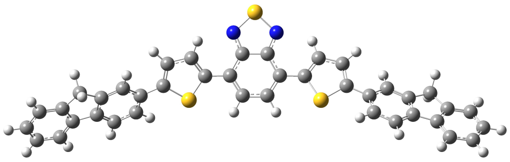

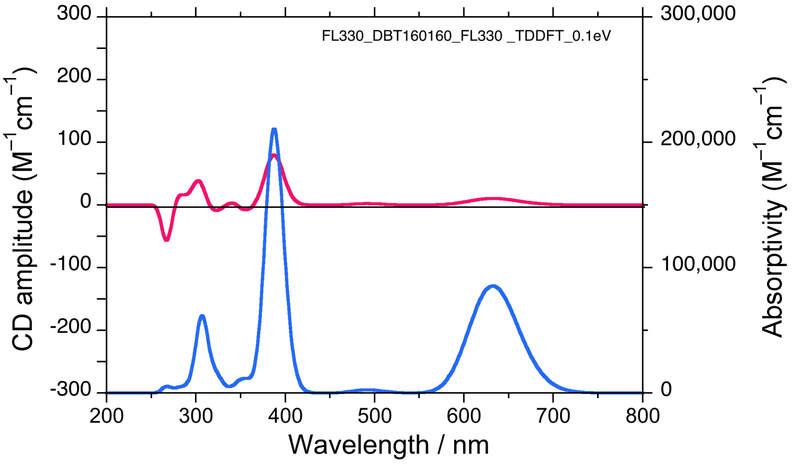

Figure S26. The simulated CD and UV-vis diagram of **FL330°-DBT160°-160°-FL330°** of anti-anti **FDBTF** rotamer.

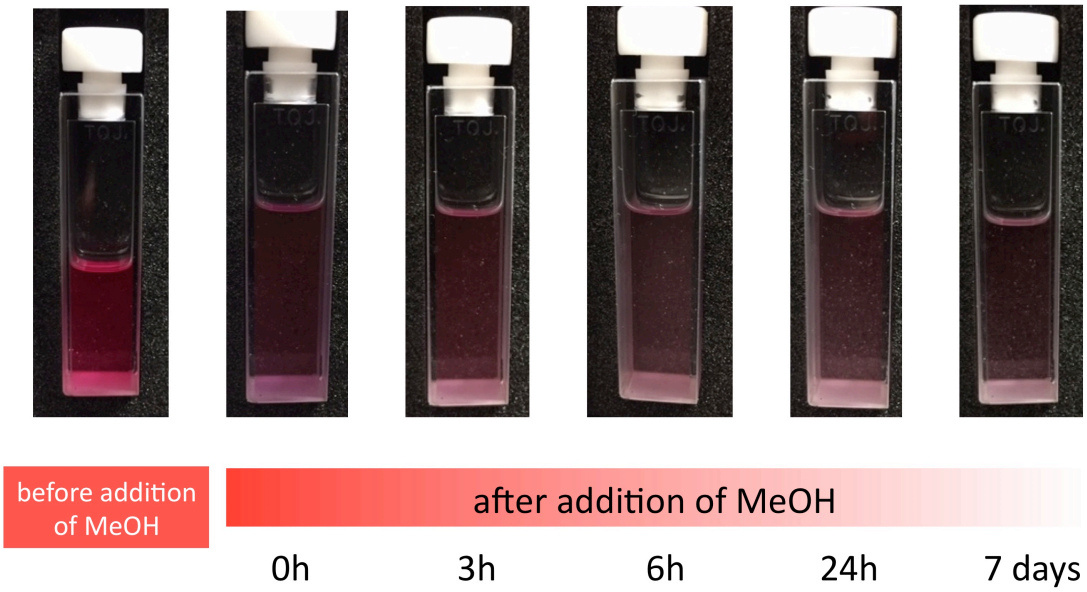

Figure S27. Time-course change in reddish colour of **PF8DBT** hetero-aggregate with **PSi-*S*** (1/1 in molar ratio as of repeating unit). ([**PF8DBT**]$_0$ = [**PSi-*S***]$_0$ = 3 x 10^{-5} M, path length of 1.0 cm in $CHCl_3$: MeOH = 2/1 (v/v) at room temperature.

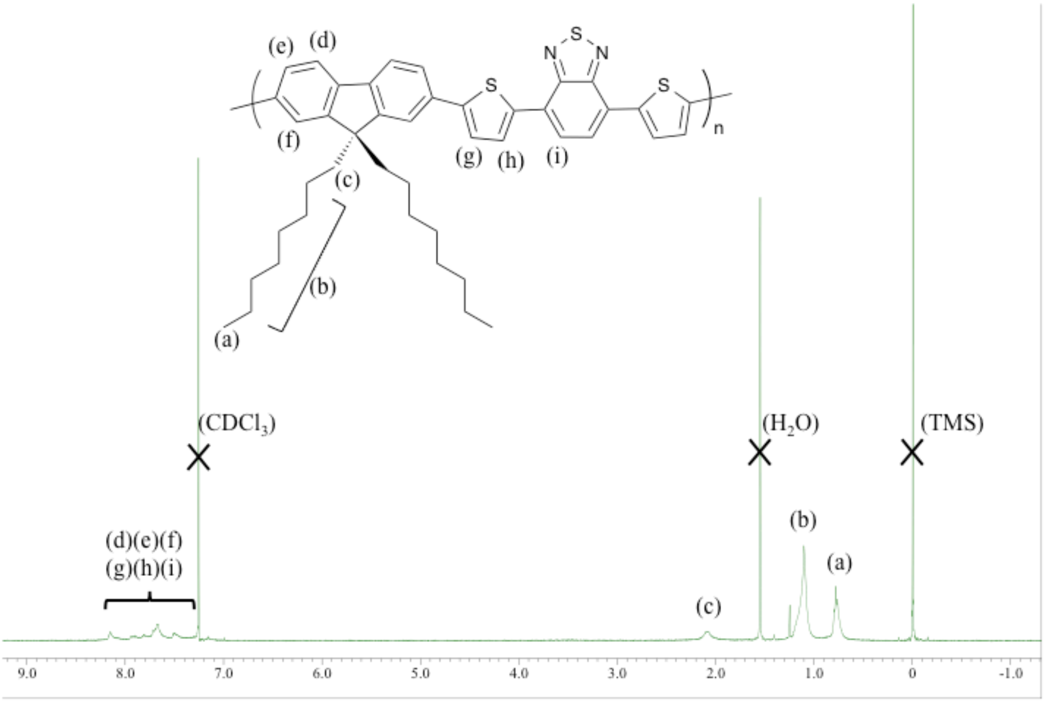

Figure S28. ^{1}H-NMR spectrum of the fractionated **PF8DBT** sample used in this work in $CDCl_3$, while the raw polymer was provided from Aldrich.

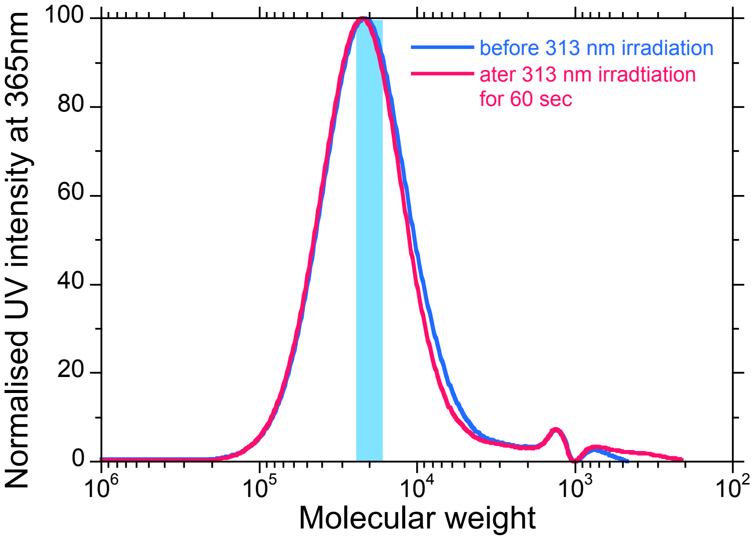

Figure S29. GPC charts (monitored at 365 nm) of the fractionated **PF8DBT** in chloroform solution before and after UV (313-nm) irradiation for 60 sec. Before the irradiation, *Mw* = 24900, *Mn* = 15400, *PDI* = 1.62, after the irradiation, *Mw* = 25900, *Mn* = 15400, *PDI* = 1.50. **PF8DBT** had no remarkable degradation for the short-period UV irradiation.

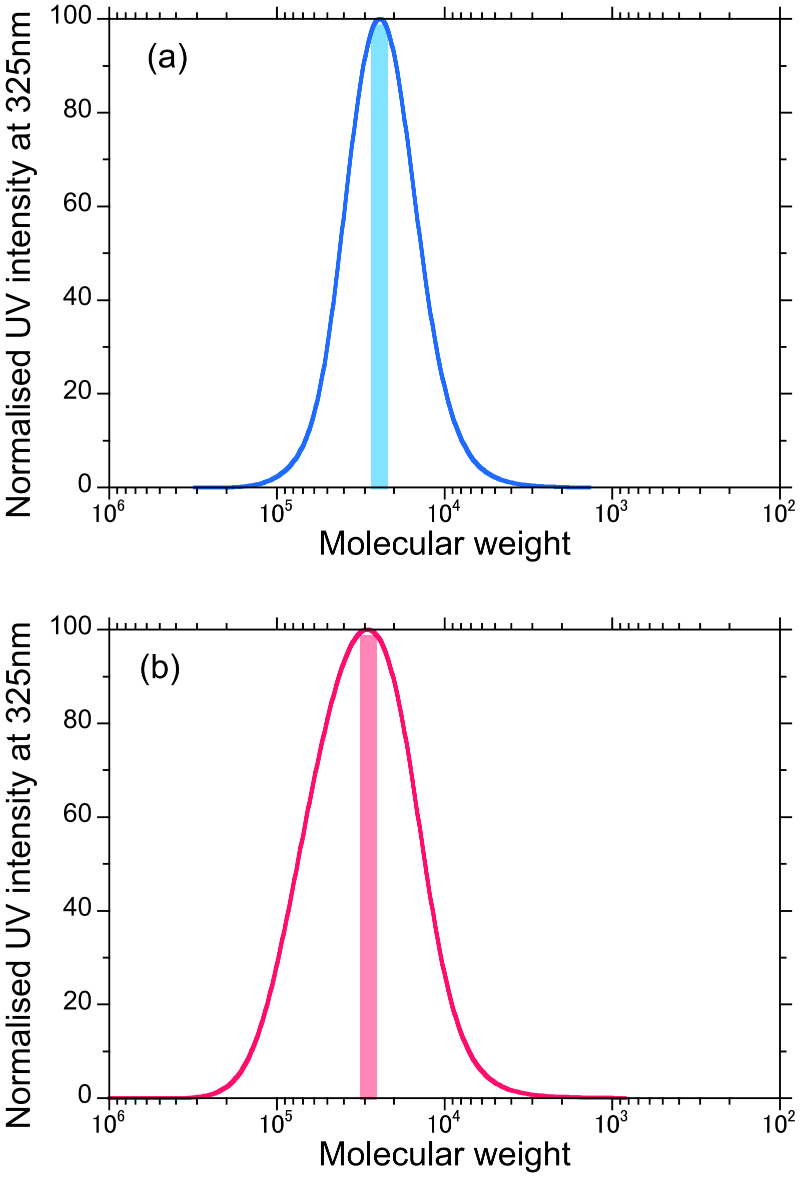

Figure S30. GPC charts (monitored at 325 nm) of (a) **PSi-*S*** and (b) **PSi-*R*** before UV (313-nm) irradiation. **PSi-*S***: *Mw* = 26900, *Mn* = 20400, *PDI* = 1.31, **PSi-*R***: *Mw* = 39200, *Mn* = 23900, *PDI* = 1.64.

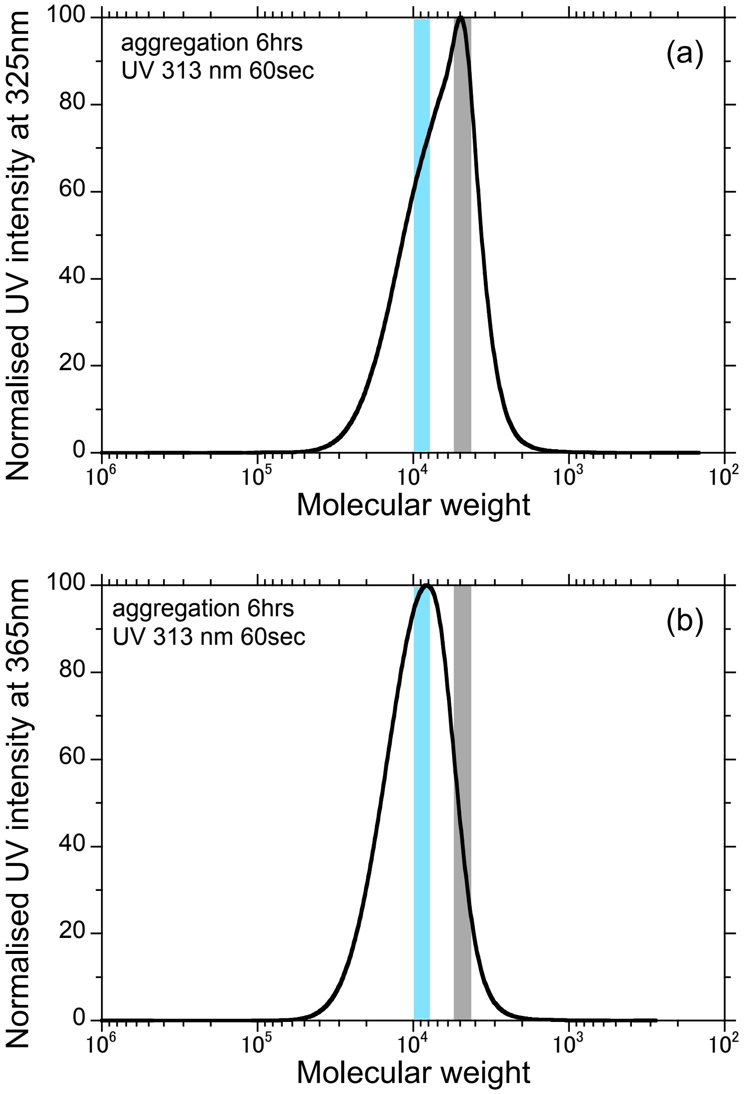

Figure S31. GPC charts monitored at (a) 325 and (b) 365 nm) of **PF8DBT-and-PSi-*S*** hetero-aggregate (1:1 in molar ratio) in chloroform/methanol (= 2/1 (v/v)) with an ageing time of 6 hrs, followed by UV (313-nm) irradiation for 60 sec.

Soluble diorgano-polysilanes are efficient positive-type, resist materials upon exposure to UV light and e-beam sources (R. D. Miller and J. Michl, *Chem. Rev*., 1989, **89**, 1359-1410). In the case of positive-type, polymeric resist materials, the decomposed low molecular weight species are readily soluble in common organic solvents and can be removed via rinsing with alcoholic solvents at room temperature. The photocleaved, low molecular weight species of dialkylpolysilanes are readily dissolved in a mixture of chloroform/methanol (2/1, v/v). The cleaved, low molecular weight species of **PSi-(*S*)** in a reaction mixture do not have the Siσ-Siσ^* band at 310 – 320 nm (Figs. 4a and 4c). The broader single-sign Cotton bands at 310 – 320 nm arise from the π–π^* bands of **PF8DBT**.

Low molecular weight dialkylpolysilanes smaller than $M \approx 2000 - 3000$ are readily soluble in methanol and ethanol when a work-up purification process is used for the as-prepared polysilane dissolved in toluene. Low molecular weight polysilane species are removable using alcoholic chloroform. Most of the photocleaved fragments of the polysilanes diffuse to the surrounding solvent, and a small portion of the low molecular weight polysilanes may remain in the aggregates, based on additional GPC measurements of several samples.

Initially, we confirmed that the photodegradation degree of **PF8DBT** upon short-term UV-irradiation is minimal because the GPC charts of **PF8DBT** in a pure $CHCl_3$ solution in a quartz cuvette were unchanged before and after irradiation at 313 nm (ESI, Fig. S29). Also, the GPC charts of **PSi-(*S*)** and **PSi-(*R*)** in a pure THF solution had single peak molecular weights at ≈ 25,000 and ≈ 30,000, respectively (ESI, Fig. S30).

We prepared **PF8DBT**-**PSi-(*S*)** hetero-aggregates dispersed in $CHCl_3$-methanol (2:1 (v/v) with an ageing time of 6 h), followed by irradiation at 313 nm for 60 s in a quartz cuvette. The GPC chart responsible for the π–π* transition of **PF8DBT** was monitored at 365 nm and had a monomodal signal, meaning a peak molecular weight at ≈ 9000 (ESI, Fig. S31). The GPC chart monitored at 325 nm had one shoulder signal at ≈ 9000 (the π–π* transition of **PF8DBT**) and one peak signal at ≈ 4000, which is the σ–σ* transition of a trace amount of **PSi-(*S*)** in the cosolvent (ESI, Fig. S31). The marked decrease in the peak molecular weight of the polysilanes after 60 s of UV irradiation is obvious.

The photoscissored, low molecular weight fragments without Siσ-Siσ* signals at 325 nm readily diffused into the surrounding cosolvent. A small portion of the lower molecular weight polysilanes may remain in the aggregates. If we used a shorter UV wavelength (a higher energy source) (*e.g.*, 254 nm), the UV wavelength selective decomposition of the lower molecular weight polysilanes is feasible. We proved that UV wavelength selective photoscissoring experiments of bisignate optically active polysilane are feasible using the UV-light source of a CD spectrometer (M. Fujiki, *J. Am. Chem. Soc.*, **116**, 11976-11981 (1994).

Table S1. Population analysis of eight possible **FDBTF** rotamers relative to the most stable **FL30°-DBT160°160°-FL30°** rotamer in a vacuum.

Structure	Energy	λ_{max}	population (%)
FL30°-DBT30°30°-FL30°	E= +3.13 kcal/mol	615.2 nm	0.16
FL150°-DBT30°30°-FL150°	E= +2.95 kcal/mol	620.8 nm	0.22
FL210°-DBT30°30°-FL210°	E= +3.21 kcal/mol	618.0 nm	0.14
FL330°-DBT30°30°-FL330°	E= +2.93 kcal/mol	616.6 nm	0.23
FL30°-DBT160°160°-FL30°	E= 0.00 kcal/mol	636.2 nm	34.9
FL150°-DBT160°160°-FL150°	E= +0.36 kcal/mol	633.4 nm	18.8
FL210°-DBT160°160°-FL210°	E= +0.28 kcal/mol	636.2 nm	21.6
FL330°-DBT160°160°-FL330°	E= +0.22 kcal/mol	632.0 nm	22.8